Published in final edited form as:
J Neurophysiol. 2006 June ; 95(6): 3449–3459. doi:10.1152/jn.00823.2005.

Serotonergic modulation of inspiratory hypoglossal motoneurons in decerebrate dogs

Ivo F. Brandes[1,2], **Edward J. Zuperku**[1,2], **Astrid G. Stucke** [1,2], **Danica Jakovcevic**[1,2], **Francis A. Hopp**[1,2], and **Eckehard A. Stuth**[1,2,3]

1*Department of Anesthesiology, Medical College of Wisconsin, Milwaukee, WI,*

2*Clement J. Zablocki VA Medical Center, Milwaukee, WI, and*

3*Children's Hospital of Wisconsin, Pediatric Anesthesia, Milwaukee, WI*

Abstract

Inspiratory hypoglossal motoneurons (IHMNs) maintain upper airway patency. However, this may be compromised during sleep and by sedatives, potent analgesics, and volatile anesthetics by either depression of excitatory or enhancement of inhibitory inputs. *In vitro* data suggest that serotonin (5-hydroxytryptamine, 5-HT), via the 5-HT_{2A} receptor subtype, plays a key role in controlling the excitability of IHMNs. We hypothesized that *in vivo* 5-HT modulates IHMNs activity via the 5-HT_{2A} receptor subtype. To test this hypothesis, we used multibarrel micropipettes for extracellular single neuron recording and pressure picoejection of 5-HT or ketanserin, a selective 5-HT_{2A} receptor subtype antagonist, onto single IHMNs in decerebrate, vagotomized, paralyzed, and mechanically ventilated dogs. Drug-induced changes in neuronal discharge frequency (F_n) and neuronal discharge pattern were analyzed using cycle-triggered histograms. 5-HT increased the control peak F_n to 256 % and the time-averaged F_n to 340 %. 5-HT increased the gain of the discharge pattern by 61 % and the offset by 34 Hz. Ketanserin reduced the control peak F_n by 68 %, the time-averaged F_n by 80 %, and the gain by 63 %. These results confirm our hypothesis that *in vivo* 5-HT is a potent modulator of IHMN activity via the 5-HT_{2A} receptor subtype. Application of exogenous 5-HT shows that this mechanism is not saturated during hypercapnic hyperoxia. The two different mechanisms, gain modulation and offset change, indicate that 5-HT affects the excitability as well as the excitation of IHMNs *in vivo*.

Introduction

Hypoglossal motoneurons (HMNs) innervate all tongue muscles, including the genioglossal muscle, the main protruder of the tongue, and thus contribute significantly to the maintenance of upper airway patency during inspiration (Miki et al. 1989). Partial or complete loss of inspiratory HMN (IHMN) activity during sleep (Remmers et al. 1978), during various stages of anesthesia (Eastwood et al. 2002), or during post-anesthetic recovery (Dhonneur et al. 1999), can lead to upper airway obstruction with resulting hypoxia. HMNs are thought to receive inputs from several regions within the brain. In rats, serotonergic and peptidergic raphe neurons project to HMNs (Manaker and Tischler 1993; Takeuchi et al. 1983), as well as noradrenergic neurons that originate from the locus subceruleus (Aldes et al. 1992). Sleep-wake states as well as rhythmic motor activities, including breathing, influence the magnitude of these neuronal inputs (Jacobs and Azmitia 1992; Veasey et al. 1995). In decerebrate cats, serotonin (5-hydroxytryptamine, 5-HT) seems to provide substantial tonic excitatory drive to

Corresponding author: Eckehard A. E. Stuth, MD, Research Service 151, Clement J. Zablocki VA Medical Center, 5000 West National Avenue, Milwaukee, WI 53295, (414) 384-2000 ext. 41579, estuth@mcw.edu.

various types of HMNs (Kubin et al. 1992). Kubin et al. demonstrated in decerebrate cats during experimentally induced REM-like sleep that reduced levels of endogenous 5-HT and depression of hypoglossal activity are closely linked (Kubin et al. 1994). Increased levels of 5-HT are released during wakefulness, when raphe neurons are active, and may increase HMN activity; whereas, withdrawal of 5-HT, in particular during REM sleep when raphe neurons are inactive, may decrease HMN activity. This decreased activity is thought to contribute to the loss of muscle tone in the tongue and to compromise upper airway patency (Jacobs and Azmitia 1992).

However, the contribution of endogenous 5-HT to the physiological activity of single IHMNs has not been characterized in an *in vivo* preparation. *In vitro* studies show that activation of HMNs by 5-HT is mediated by postsynaptic neuronal 5-HT_{2A} receptors (Fenik and Veasey 2003; Schwarzacher et al. 2002). One identified mechanism of action is a decrease in a leak K^+ channel conductance (Bayliss et al. 1997; Sirois et al. 2002) that leads to increased excitability of the neuronal cell membrane.

We hypothesize that the discharge activity of IHMNs *in vivo* depends on endogenous 5-HT and is mediated by postsynaptic 5-HT_{2A} receptors. We tested this hypothesis in a decerebrate dog model by characterizing the effects of exogenous 5-HT as well as endogenous 5-HT, via a selective 5-HT_{2A} block with the antagonist ketanserin, on single IHMNs with a special focus on changes in the discharge pattern.

Material and Methods

Animal Preparation and General Methodology

This research was approved by the Medical College of Wisconsin Animal Care Committee and conformed to standards set forth in the National Institutes of Health Guide for Care and Use of Laboratory Animals. Anesthesia was induced in dogs by mask with isoflurane. They were intubated with a cuffed endotracheal tube, and from then on mechanically ventilated with oxygen. Isoflurane (1.3–1.8 MAC) was applied throughout the surgical procedures and only discontinued after completion of decerebration (1 MAC isoflurane in dogs = 1.4% (Kazama and Ikeda 1988)). The animals were positioned in a stereotactic device (model 1530; David Kopf Instruments, Tujunga, CA) with the head ventrally flexed (30 degrees). Bilateral neck dissections were performed. Superficial muscles of the region were retracted, and the hypoglossal nerve was separated from its surrounding tissue. The hypoglossal nerve was exposed, cut near the bifurcation point of lateral and medial branches, desheathed, and placed onto a custom made electrode for recording. This electrode was custom made by cutting a 1 cc tuberculin syringe (Terumo Syringe, Terumo Medical Cooperation, Elkton, MD) longitudinally in half, placing two 80 μm thick teflon-coated stainless steel wires through the bottom of a trough and forming two loops of bare wire. The proximal end of the nerve was placed through the wire loops and covered with silicon gel to provide a barrier to blood and prevent drying of the nerve. The C5 phrenic nerve rootlet was desheathed and placed onto a custom made hook electrode for recording. Bilateral vagotomy was performed to achieve peripheral deafferentation from pulmonary stretch receptor input. This avoids volume feedback from the mechanical ventilation via vagal inputs to the respiratory centers. Bilateral pneumothorax was performed to minimize brainstem movement and eliminate phasic inputs from chest wall afferents. The animals were decerebrated at the midcollicular level (Tonkovic-Capin et al. 1998) and only then paralyzed with pancuronium (Baxter Healthcare Corporation, Deerfield, Ill) (bolus of 0.1 mg/kg, followed by 0.1 $mg \cdot kg^{-1} \cdot h^{-1}$). For single neuron recording, an occipital craniotomy was performed to expose the dorsal surface of the medulla oblongata. Dexamethasone (American Regent Laboratories, Shirley, NY) was administered intravenously to prevent brain swelling (1 mg/kg after anesthesia induction and every 6 h thereafter). A heating blanket was used to maintain esophageal temperature at 38.5 ± 1 ºC. Mean arterial

pressure was kept at or above 100 mmHg and protocols were performed only during steady state conditions for blood pressure. In this study, no vasopressor support was necessary to maintain stable hemodynamics. To minimize blood loss through the activation of the fibrinolytic system secondary to the surgical trauma (Nilsson et al. 1960; Risberg 1978), ε-amino-n-caproic acid (Sigma-Aldrich Co., St. Louis, MO) was administered intravenously (bolus of 125 mg/kg at the beginning of surgery, followed by 15 $mg \cdot kg^{-1} \cdot h^{-1}$).

Neuron Recording Technique, Data Collection and Experimental Conditions

For recording, we used anatomical information from a previous study as a guide for locating IHMNs. The cholera toxin B subunit, injected into the genioglossus muscle of adult mongrel dogs, was used to retrogradely label genioglossal motoneurons, which comprise the largest subgroup of IHMNs. These IHMNs are distributed within a compact column, extending from 0.5 mm caudal to 3.5 mm rostral to obex. They are located at a mean depth of 1.24 mm (SD 0.46) and centered at about 0.98 mm (SD 0.12) lateral from the midline (Brandes et al. 2004a). Custom made multibarrel compound glass micropipettes, consisting of a recording barrel containing a 7-micrometer carbon filament and three drug barrels, were used to simultaneously record extracellular neuronal activity of an adequately identifiable single IHMN before and during pressure ejection of serotonin (5-HT) or ketanserin onto the neuron. 5-HT (0.5 mM) was dissolved in an artificial cerebrospinal fluid (aCSF) (Stuth et al. 2000). Ketanserin was first dissolved in DMSO to a concentration of 20 mM, which was subsequently diluted to 500 micromolar with aCSF that had previously been adjusted to a pH of ~6.0. Although freshly mixed drugs were used in these experiments, refrigerated aliquots of ketanserin have been shown to remain in solution for more than a month. The effects of the acidified aCSF vehicle on IHMNs had been found to be negligible in pilot studies (unpublished observations by authors, 2003).

Picoejection Technique—The pressure microejection system used in this study is similar to the “Picospritzer” (General Valve Corp., Fairfield, NJ) in that each timed pressure pulse ejects a volume in the 40–400 pl range. However, by delivering repeated picospritzes of micromolar solutions of agents, typical dose rates in the picomole/minute range can be delivered. The parameter ranges used to alter dose rates were ejection pressure: 10–100 psi; pulse duration: 10–100 msec; and frequency of the ejection pressure pulses: 0.2–2 Hz. Ejected dose rate (volume/time) was measured via height changes of the meniscus in the pipette barrel with a 100 times magnification microscope equipped with a reticule (resolution ~2 nl). To obtain steady-state dose-response data, constant-rate picoejection was used, and dose rates were mainly increased via changes in ejection pulse rate. Using this approach, it is possible to produce quasi steady-state drug concentrations at given distances from the pipette tip due to the properties of diffusion. Increasing the rate of ejection increases the concentration at any given distance. The maximum achievable concentration is the barrel concentration.

Recorded Variables—Single unit extracellular IHMN activity, hypoglossal and phrenic nerve activities, picoejection marker pulses, endtidal CO_2, systemic blood pressure, and airway pressure were recorded on a digital tape system (model 3000A, A. R. Vetter Co., Rebersburg, PA). Endtidal volatile anesthetic concentration and airway concentration of inspiratory and expiratory O_2 and CO_2 were monitored with a POET IQ Anesthesia Gas Monitor (Criticare Systems, Inc., Waukesha, WI). These variables, or their time-averages, and a rate-meter output of discharge frequency (100 ms bins) were also continuously displayed on a computerized chart recorder (ADInstruments, Powerlab/16SP, Castle Hill, Australia). Online spike-triggered averaging (STA) was used to confirm that the recorded action potentials originated from a hypoglossal motoneuron. The presence of an axon spike potential within the hypoglossal nerve activity (e.g., Fig. 1) and the neuron firing in phase with the phrenic nerve activity, confirmed that the recorded brainstem neuron was an IHMN. The tape-recorded data were digitized and

analyzed off-line. Timing pulses at the beginning and end of neural inspiration were derived from the phrenic neurogram and were used to determine the respiratory phases. Cycle-triggered histograms, triggered by the timing pulse at the onset of phrenic nerve activity, were used to quantify the neuronal discharge frequency.

The protocols were performed under both steady state hyperoxic and hypercapnic conditions (fraction of inspired oxygen [FiO_2] > 0.6, arterial oxygen tension [PaO_2] > 300 mmHg, arterial carbon dioxide tension [$PaCO_2$] 55–65 mmHg). The exact level of $PaCO_2$ varied within those limits from animal to animal, but was kept constant within an animal once strong phasic phrenic activity was obtained; great care was taken to keep the $PaCO_2$ tightly controlled within each neuron protocol by keeping artificial ventilation and ventilator fresh gas flows constant, by closely monitoring end-tidal CO_2 trends, and by intermittent blood gas sampling. Hypercapnia was used to increase excitatory drive to the respiratory centers, which provided robust phrenic nerve activity and inspiratory hypoglossal nerve activity under baseline conditions. This was necessary because other drive inputs to hypoglossal motor neurons such as peripheral chemodrive and phasic inputs from negative pressure sensitive upper airway receptors were abolished by hyperoxia and intubation with positive pressure ventilation, respectively (Anderson et al. 1990). The experimental protocol consisted of picoejection of the agonist or antagonist at increasing incremental dose rates. Following picoejection, recovery to baseline discharge frequency was awaited for every neuron. The lack of effect of the aCSF vehicle was periodically confirmed in separate runs. To avoid confusion from residual effects of serotonin on the measurement of endogenous levels of serotonin, we also performed all experiments with the antagonist ketanserin in a separate group of animals (see protocol 2). However, to demonstrate that ketanserin is a competitive antagonist of serotonin in our setup, we additionally performed a small number of agonist-antagonist studies on single neurons.

Protocol 1: Effects of exogenous serotonin on the spontaneous neuronal discharge frequency

The IHMN discharge frequency (F_n) was measured for 10–15 respiratory cycles during a control period, at each dose rate, and after recovery. 5-HT was pressure picoejected at increasing dose rates onto single neurons. Typically, dose rates were held constant for 2–5 minutes to obtain a quasi steady-state discharge pattern before increasing the dose rate to the next higher level. Dose rates were increased until no further increase in peak F_n was observed, but before background activity became too intense to adequately discriminate the neuron. Picoejection durations of 10–15 min with two to three different dose rates were feasible. Sufficient time was allowed for peak F_n to return to the control level. This typically required 45–60 minutes.

Protocol 2: Effects of the 5-HT_{2A} antagonist ketanserin on the spontaneous neuronal discharge frequency

For the control period and at each dose rate, the neuronal discharge activity from 10–15 respiratory cycles was averaged to obtain mean values for the peak F_n and average F_n during the inspiratory phase for each condition as in protocol 1. After establishing a stable baseline, peak F_n was measured during a pre-ejection control period (F_{con}). Then ketanserin was applied in increasing dose rates until an increase in picoejection dose rate did not result in any further decrease in peak F_n. In some neurons with relatively low F_{con}, the maximum effect could not be determined because it was below the discharge threshold. In these neurons, picoejection was stopped before neuronal activity was completely silenced since the presence of neuronal activity is a prerequisite to assess changes in the discharge pattern. Typically, picoejection durations of 10–15 min with three dose rates were needed. Sufficient time was allowed for peak F_n to return to the control level. This typically required 30–45 minutes. To obtain an

accurate estimate of the endogenous serotonin level, we avoided using exogenous serotonin due to its possible long-lasting effects.

Protocol 3: Effects of CO_2 on hypoglossal and phrenic nerve activities

In five dogs, the activities of hypoglossal (XII) and phrenic nerves were initially obtained during moderate hypercapnia. The tidal volume of the ventilator was then increased to lower end-tidal CO_2 ($ETCO_2$) to the level at which phasic inspiratory-related XII nerve activity decreased to zero. After a period of stabilization (~10 minutes), CO_2 gas was gradually added via a flow meter on the anesthesia machine to the inspired hyperoxic gas mixture without changing the mechanical ventilator settings. This produced graded increases in $ETCO_2$ to a maximum level of ~65 mmHg. The time-averaged peak XII and phrenic nerve activities were analyzed in terms of $ETCO_2$ to determine the "apneic" thresholds and saturation levels for both activities.

Data analysis

Cycle-triggered histograms (CTHs) based on 10–15 respiratory cycles were used to quantify the peak and time-averaged neuronal discharge frequency before and during application of 5-HT or ketanserin, respectively. The time-averaged F_n was calculated as the sum of the CTH bins (50 ms each) during the inspiratory phase T_I divided by the duration of the inspiratory phase (e.g., Fig. 2A, vertical dashed lines). In order to compare data from animal to animal, the data were normalized with respect to the control peak F_n and time-averaged F_n of each single neuron protocol, which was assigned a value of 100%. Since the 5-HT and ketanserin picoejection protocols were performed in different groups of animals, only the control condition was common to both sets of experiments. In order to allow comparison between the two data sets in both experiments, we normalized to this common control condition rather than the largest value for each experiment. The control condition for the ketanserin runs was always the largest value for these experiments, but the same control condition for the serotonin runs was always the smallest value for these runs but of the same magnitude as the control for the ketanserin runs.

Time-synchronized plots of the control discharge pattern (F_{con}) vs. the discharge pattern during drug application (F_n (drug)) were used to analyze the relationship between the two patterns. This method of analysis is independent of the time-course of the discharge frequency pattern. Such plots are typically linear, where a change in the regression slope indicates a change in gain and a change in intercept indicates a change in tonic activity. A plot of the control pattern against itself results in a line (line of identity: LOI) with a slope of 1 and an intercept of zero. For statistical purposes, the slope is expressed as the percent change from a value of one, while the intercept is compared to zero, and a paired-t analysis is used (e.g., Fig. 2B).

Normal distribution of the data was confirmed with the Kolmogorov-Smirnov test, and data were then tested for significant differences with Student's t-test. All values are given as mean and standard deviation (SD), and $p < 0.05$ was used to indicate significant differences unless stated otherwise.

Results

The IHMNs recorded in this study were found in a region from 0.25 mm caudal to 2.0 mm rostral to obex, at a mean depth of 2.75 mm (SD 1.11), and centered 1.16 mm (SD 0.31) lateral from the midline. All IHMNs started firing with the onset of the phrenic nerve activity or shortly thereafter and exhibited an incrementing discharge pattern.

Protocol 1: Effects of exogenous serotonin on the spontaneous neuronal discharge frequency

28 neuron protocols were obtained in 16 dogs. The mean peak F_{con} was 42 Hz (SD 21), and the mean time-averaged F_{con} 19 Hz (SD 11). Increasing dose rates of 5-HT always resulted in a gradual increase in F_n (e.g., Fig. 3). At intermediate dose rates, the neurons fired throughout the whole inspiratory phase, while at the maximal effective dose rate, the neurons also showed activity during the previously silent expiratory phase. Analysis of the $F_{5\text{-}HT}$ vs. F_{con} plots (e.g. Fig. 2B, lower) indicated that 5-HT-mediated increase in inspiratory phase activity was mainly due to an increase in the plot slope (gain) relative to the line-of-identity (LOI) and to a smaller degree the y-intercept. This increase in gain is also reflected by increases in the CTH slopes during 5-HT application (e.g., Fig 2B, Upper). However, at the highest 5-HT dose rates, tonic activity appeared during the previously silent expiratory phase, and contributed to the discharge pattern (e.g., Fig. 3 lower right). The normalized data showed that 5-HT, at maximally effective dose rates (16 pmol/min (SD 24)), increased the time-averaged F_n to 340 % (SD 140) ($p < 0.001$, Fig. 4, left) and the peak F_n to 256 % (SD 79) ($p < 0.001$, Fig. 4, right) relative to baseline. At maximal dose rates, the gain of the discharge patterns as measured by the slope for the $F_{5\text{-}HT}$ vs. F_{con} plots was increased by 61 % (SD 89) ($p < 0.001$, Fig. 5, left) and the offset by 38 Hz (SD 26) ($p < 0.001$, Fig. 5 right).

Protocol 2: Effects of the 5-HT_{2A} antagonist ketanserin on the spontaneous neuronal discharge frequency

21 neuron protocols were obtained in nine dogs. Again, during control conditions the IHMNs exhibited only phasic inspiratory activity, as indicated by the neuron firing in phase with the phrenic nerve. The peak F_{con} was 53 Hz (SD 20) and the time-averaged F_{con} 18 Hz (SD 11). Stepwise increases in ketanserin dose rates resulted in a stepwise decrease in F_n (Fig. 6). At higher dose rates a ceiling effect was noted in 13 of 21 neurons, i.e., an increase of ketanserin did not decrease F_n any further. Normalization of the data showed that ketanserin at the maximally effective dose rate (14 pmol/min (SD 8)) decreased the time-averaged F_n by 80 % (SD 15) and the peak F_n by 68 % (SD 15) ($p < 0.001$, Fig. 4). The second step of the analysis was the evaluation of ketanserin-induced changes in the neuronal discharge pattern. Since a ceiling effect of the ketanserin response was not essential in determining the quality of the changes, and the results for the two neuron groups for slope and offset were not significantly different (data not shown), we pooled the data from all 21 neurons. Ketanserin reduced the gain as measured by the slope for the F_{KET} vs. F_{con} plots by 63 % (SD 24) ($p < 0.001$, Fig. 5, left) and reduced the offset by 4 Hz (SD 9) ($p < 0.06$, Fig. 5, right).

Ketanserin as a competitive serotonin antagonist—The ability of ketanserin to act as a competitive antagonist of exogenous 5-HT was confirmed in a small number of additional protocols by studying agonist and antagonist on the same IHMN. An example of this competitive antagonism is given in Fig. 7, where picoejection of 5-HT produced an increase in phasic activity during the inspiratory phase at low concentrations and an additional increase in activity during expiratory phase at higher concentrations (e.g., Fig.7 left; HMN spike activity). To adequately quantify these 5-HT effects, the average discharge frequency (ave F_n) during each full respiratory cycle was calculated, which includes activity during both phases. A plot of ave F_n (Fig. 7, left 2nd trace) vs. the estimated dose rate dependent relative serotonin concentration (Fig. 7, left, 1st trace) is shown in Fig. 7, lower left, for the initial run (S1). The ave F_n saturated at the highest serotonin concentrations. Since only picoejection dose rate can be measured, the concentration profile is an approximated estimate based on theoretical models for diffusion from a point source, i.e., the tip of the micropipette. The concentration profile reflects the time-dependent increase that occurs when picoejection is initiated and maintained constant. The steady-state concentration is quasi-linearly related to the ejection dose rate. At high dose rates the concentration can approach the micropipette barrel

concentration, but this is also dependent on distance from the tip. Following recovery from 5-HT run S1, ketanserin was then picoejected on the neuron and reduced ave F_n to zero (Fig. 7, right lower, run K1). During this ketanserin block a higher dose rate of 5-HT was required to overcome the competitive antagonism as seen by the right shift of the second 5-HT dose-response curve (Fig. 7, left lower, run S2). While maintaining the peak dose rate, ketanserin was again picoejected, but a higher dose rate was required to antagonize the 5-HT effects as seen by the right shift of the second ketanserin dose-response curve (Fig. 7, right lower, run K2). Immediately after termination of ketanserin ejection (run K2), its antagonism was reversed by yet a higher 5-HT ejection dose rate, where ave F_n reached its maximum discharge rate (~20 Hz). Picoejection of ketanserin at a yet higher dose was again required to overcome the 5-HT effect (run K3). The dose rates for runs K2 and K3 were not increased enough to produce complete reduction in ave F_n, due to concerns about losing the neuronal activity during these ejection maneuvers at higher ejection rates. However, once the final 5-HT ejection was terminated, the latent effects of ketanserin led to a transient silencing of the neuron, which was followed by a gradual recovery from the antagonist effects. These results demonstrate that both drugs appear to antagonize each other in a competitive manner at and even above the dose rates that were typically used in protocols 1 and 2.

Protocol 3: Effects of CO_2 on hypoglossal and phrenic nerve activities

To characterize the effects of decerebration, paralysis and mechanical ventilation on the apneic thresholds of both XII and phrenic nerve activities and to define the effects of CO_2 drive levels to produce adequate IHMN activity, the CO_2 dose-response characteristics of the XII and phrenic nerve activities were studied in five dogs. An example of the effects of increasing CO_2 levels on phrenic and XII activities are shown in Fig. 8, upper, along with the corresponding plot of normalized peak activity vs. $ETCO_2$ (Fig. 8, left lower). Nonlinear regression, using a hyperbolic function (general form: $Y=X^3/(X^3+X_o^3)$, where Y is peak F_n and X is $ETCO_2$), was used to fit both activity plots and to aid in extrapolating the apneic thresholds especially for phrenic activity, since $ETCO_2$ was decreased only to the point where XII activity could no longer be observed. The response curve for XII activity is right-shifted and shallower with a greater linear range than that for the phrenic activity. The apneic thresholds were ~38 and ~42 mmHg for the phrenic and XII activities, respectively, and an $ETCO_2$ of ~52 mmHg was required to produce a peak XII activity of 50% of maximum. The XII nerve activity vs. $ETCO_2$ plots for five dogs and group mean curve are given in Fig. 8, middle lower. In three of five animals there was no XII activity below an $ETCO_2$ of 42 mmHg. The mean curves ± 1 SE bands of both activities are given in the right lower of Fig. 8. The XII curve was consistently right shifted and shallower than the phrenic response curve. $ETCO_2$ levels of 65–70 mmHg were required to produce maximal XII activity. $ETCO_2$ levels required for 50% of maximum ranged from 41–55 mmHg (Fig. 8, middle lower).

Discussion

This study demonstrates for the first time *in vivo* the effect of exogenous and endogenous 5-HT on the neuronal discharge pattern of single IHMNs and confirms the significant role of 5-HT in the control of IHM neuronal activity. Our data show that both exogenous and endogenous 5-HT powerfully gain modulate the discharge patterns of IHMNs primarily via postsynaptic $5\text{-}HT_{2A}$ receptors, based on the ketanserin results. We cannot rule out a possible presynaptic effect of picoejected serotonin on the IHMN response due to presynaptic $5\text{-}HT_{1A}$ or $5\text{-}HT_{1B}$ receptors, which are inhibitory. However, the overall response to serotonin was excitatory and may have masked a presynaptic effect. Furthermore, serotonergic modulation seems so effective that antagonism of $5\text{-}HT_{2A}$ receptors in a subgroup of neurons can completely silence neuronal activity.

Several studies have shown that 5-HT excites HMNs *in vitro* (Bayliss et al. 1997; Schwarzacher et al. 2002) as well as *in vivo* (Fenik et al. 1997; Jelev et al. 2001; Sood et al. 2003). Fenik and Veasey demonstrated with *in vivo* injections of antagonists selective for serotonin receptor subtypes 2A, 2C, or 7 into the hypoglossal motor nucleus in rats that the 5-HT_{2A} receptor was the predominantly active 5-HT receptor subtype on IHMNs (Fenik and Veasey 2003). The 5-HT_{2C} receptor subtype showed rapid desensitization, and there was no evidence of 5-HT_7 receptor subtype activity. Antagonism of the 5-HT_{2A} receptor subtype with MDL 100,907 depressed the ipsilateral hypoglossal motor nerve activity by 61% (Fenik and Veasey 2003). Our study similarly shows a profound depression of single IHMN activity by ketanserin. Considering that IHMNs also receive substantial glutamatergic excitatory drive (unpublished observation, Astrid G. Stucke, MD, Medical College of Wisconsin, Milwaukee, WI, March 2003) our findings suggest that the mechanism of action of 5-HT may be to alter membrane excitability rather than simply to increase excitatory drive. This is confirmed by the discharge pattern analysis of the effects of 5-HT_{2A} receptor subtype activation and antagonism, which both produce gain modulation as indicated by slope changes of the neuronal discharge pattern (e.g., Fig. 2B). In a similar *in vivo* canine preparation, we have observed two different forms of gain modulation of respiratory premotor neurons (Zuperku and McCrimmon 2002). Evidence for GABAergic gain modulation was observed during a block of $GABA_A$ receptors by bicuculline and was attributed to shunting part of the dendrosomatic excitatory current. A second source of gain modulation was observed during a block of the small conductance Ca^{2+}-activated K^+ channels with apamin and was attributed to a change in neuronal excitability due to changes in the amplitude of the spike after-hyperpolarization. In these studies, a change in the excitatory response to picoejections of a discrete amount of α-amino-3-hydroxy-5-methylisoxazole-4-propionic acid (AMPA) was used to determine if a change in excitability had occurred at the soma . An increase in the AMPA response during apamin block suggested an increase in neuronal excitability (Zuperku and McCrimmon 2002). Similar studies will be required to identify the mechanism of 5-HT action in the *in vivo* model.

In vitro studies suggest several effects of 5-HT on neuronal membrane properties. Whole-cell recordings from HMNs in a rat brainstem slice preparation indicate that 5-HT activates a barium-resistant sodium channel of relatively small amplitude, which leads to membrane depolarization (Bayliss et al. 1997). However, the main effect seems to be the G-protein mediated inhibition of a TWIK-related acid-sensitive K^+ (TASK) channel, resulting in an increase in neuronal input resistance, which would lead to amplification of other excitatory inputs (Sirois et al. 2002). This would be consistent with the role of the 5-HT_{2A} receptor subtype as a powerful modulator of neuronal discharge activity. Interestingly, in the above *in vitro* preparation, the volatile anesthetic halothane was shown to open the TASK channel, an effect that could be completely reversed with 5-HT (Sirois et al. 2002). It will be interesting to see if this antagonistic mechanism is of relevance *in vivo* where volatile anesthetics cause prominent depression of IHMNs at subanesthetic concentrations (Brandes et al. 2004b).

Gain modulation by 5-HT as well as norepinephrine (NE) has been previous observed *in vitro* using square-wave currents applied to HMNs in brainstem slice preparations (e.g., (Berger et al. 1992; Parkis et al. 1995). However, in a study where phrenic motoneurons were injected with a more physiological synaptic input current, that typically exhibits membrane potential oscillations, gain modulation was not observed with the bath application of NE (Parkis et al. 2003). The oscillatory potentials, which presumably arise from synchronous presynaptic inputs, are able to synchronize the spike discharge pattern of the HMNs. Bath application of NE did not increase the discharge frequency, but increased the duration of the discharge. It was suggested, that at the level of the motoneuron and muscle behavior, the functional consequences of the oscillations result in an increase in efficiency and protect against motor unit fatigue (Parkis 2003). However, our *in vivo* data clearly show that 5-HT increases IHMN peak F_n and ketanserin decreases it. This finding is similar to those of Fenik et al. (Fenik et al.

1997) in decerebrate cats where methysergide was the antagonist. Thus, it appears that the *in vitro* high frequency oscillation (HFO) hypothesis may not directly apply to the *in vivo* findings.

Methodological Considerations

Decerebration—We have discussed the advantages and limitations of the decerebrate preparation in previous publications (Dogas et al. 1998; Krolo et al. 1999; Krolo et al. 2000; Stucke et al. 2002; Stuth et al. 2000). The major advantage is that decerebration allows investigation of neurotransmission without the confounding effects of anesthetics on ligand gated receptors (Hara and Harris 2002) and other ion channels of the neuronal membrane (Sirois et al. 2000; Sirois et al. 2002). This seems especially important in IHMNs, which are already significantly depressed by subanesthetic concentrations of volatile anesthetics (Brandes et al. 2004b).

Effects of chemodrive—The mid-collicular decerebration may have possibly modified the chemodrive inputs to the IHMNs, resulting in a drive level that is different from that of awake animals. A previous study comparing the responses of decerebrate dogs with anesthetized dogs has demonstrated a left shift in the phrenic nerve ventilatory response and apneic threshold (24.7 vs. 37.6 mmHg) to carbon dioxide with decerebration (Nielsen et al. 1986). We have examined the phrenic and hypoglossal nerve responses to carbon dioxide in five dogs in our decerebrate setup (Fig. 8) and extrapolated the thresholds for phrenic and hypoglossal neural apnea to about 32 mmHg and 37 mmHg, respectively. Thus, the phrenic apneic threshold is very similar to that of sleeping unanesthetized dogs, which have apneic thresholds shifted about 5 mmHg left of the $PaCO_2$ (~ 37 mmHg) of normocapnic breathing (Nakayama et al. 2002). However, despite a possible left shift in the CO_2 response curve with decerebration, Fig. 8 shows that brisk phasic inspiratory hypoglossal nerve activity is rarely observed at normocapnia. In three of five animals there was no XII nerve activity below an $ETCO_2$ of 42 mmHg, and the half maximum level of peak activity occurs at ~52 mmHg. In addition, the XII nerve activity appears to increase approximately linearly with increasing carbon dioxide concentrations in the 42–55 mmHg $ETCO_2$ range. Therefore, we are constrained to study phasic inspiratory hypoglossal motor neuron activity during increased central chemodrive conditions, which we obtained with hyperoxic hypercapnia.

The functional deafferentation of peripheral chemoreceptor inputs with hyperoxia may have contributed to the smaller left shift of the CO_2 response curves and reflects the central CO_2 apneic threshold in our decerebrate preparation. A similar apneic threshold of 35.3 ± 5.6 mmHg was observed for phrenic nerve activity during hyperoxia in decerebrate cats (Iscoe et al. 1998). Even though these studies were performed during hypercapnia, it should be noted that during anesthetic recovery, hypercapnia in this range is common, and that during sleep many obstructive sleep apnea patients operate in this range. Thus, there is clinical and pathophysiological relevance to this level of hypercapnia.

Influence of other factors—Several factors may have contributed to the magnitude of the endogenous serotonin levels we estimated, where ketanserin reduced peak IHMN activity by ~68%. While serotonergic pathways appear to be functional in decerebrate preparations (Sakai et al. 2000), interruption of descending supra-collicular pathways may abolish central inhibitory regulation of raphe serotonergic neurons and may thus have increased the level of the endogenous serotonergic input to the IHMNs that we observed. The increase in spinal levels of serotonin following decerebration appears to be the main cause of muscle rigidity (Sakai et al. 2000). The elevated level of $ETCO_2$ we used may be a significant contributor to the endogenous serotonin level, since it appears that medullary raphe serotonergic neurons may function as central chemosensors (Nattie et al. 2004; Richerson 2004; Severson et al. 2003; Wang et al. 2001). In addition, the state of the preparation can strongly influence the

endogenous level of the serotonergic input to the IHMNs. These states include anesthesia, decerebration, quiet wakefulness, REM sleep, non-REM sleep (Dreshaj et al. 1998; Horner 2001; Kubin et al. 1998; Sood et al. 2005), as well as stage of development. In very young animals, exogenous serotonin inhibits IHMNs via the presynaptic inhibitory autoreceptors (e.g. 5-HT_{1B} receptors) of the serotonergic neurons (Singer et al. 1996). There is also evidence suggesting that vagotomy can increase raphe activity via a reduction in vagal afferent-mediated inhibition of the raphe neurons (Sood et al. 2005).

In the present acute experiments, we have not observed any qualitative differences on central respiratory activity by adding dexamethasone to our surgical preparation. Dexamethasone may alter neuromodulator function by affecting catecholamine biosynthesis via tyrosine hydroxylase, a rate-limiting enzyme in catecholamine biosynthesis. However, Joseph et al. showed in rats that although acute administration of 1 mg/kg dexamethasone stimulated tyrosine hydroxylase activity in the carotid body and thereby reduced the hypoxic ventilatory response, no effects from acute administration where seen in brainstem catecholamine areas (Joseph et al. 1998). Only chronic administration over 10 days affected central tryrosine hydroxylase activity. Since the peripheral chemoreceptors are already functionally denervated in our preparation, we would expect minimal effects of acute dexamethasone administration.

Picoejection—The picoejection method allows highly localized drug ejection onto the recorded neuron, which is prerequisite for unequivocal interpretation of the data. Concentrations are lower than with microiontophoresis, reducing the probability of nonspecific effects due to high local concentrations. In addition, monitoring of ejected drug volumes by direct monitoring of the meniscus of the drug barrel allows the calculation of dose-response curves for the applied substances. The limitations of this method have been previously delineated (Dogas et al. 1998; Krolo et al. 1999; Krolo et al. 2000; Stucke et al. 2002; Stuth et al. 2000). While it cannot be excluded that the picoejection response of the recorded neurons may be influenced by additional drug effects on presynaptic neurons, the importance of this contamination appears small since 1) the qualitative character of the neuronal response was consistent for all neurons studied, and 2) the response was always consistent with the expected postsynaptic effects of the drug. For example, 5-HT always increased neuronal discharge frequency, while an activation of presynaptic 5-HT_{1B} receptors could have caused an inhibition of the neuron (Singer et al. 1996). Similarly, ketanserin always decreased neuronal discharge frequency. 3) The picoejected doses did not change hypoglossal nerve activity. Concentration of a picoejected drug decreases rapidly with distance from the electrode tip. A theoretical analysis of the diffusion of a drug from a constant point source shows that the concentration decreases inversely (1/distance) with the distance from the source (Stone 1985).

Selectivity of ketanserin—While ketanserin has also been shown to antagonize adrenergic α_1 receptors, it appears to do so at much higher concentrations than those required to antagonize 5-HT_2 receptors. For example, the IC50 at 5-HT_2 receptors was found to be 0.65 nM while at α_1 receptors the IC 50 was 30.0 nM, or 46.5 times higher in isolated perfused rat tail arteries (Marwood 1994). In the present studies, the picoejection dose rates were always started a low levels and gradually increased until a maximal effect was observed. This happened over a narrow dose rate range as indicated by the data of Fig. 7. Thus, it is highly likely that the ketanserin effects were mainly due to antagonism of 5-HT. Furthermore, we were able to demonstrate that ketanserin functioned as a classical competitive antagonist as suggested by the parallel shifts in the log dose-response curves for both 5-HT and ketanserin of Fig. 7.

Notably, our *in vivo* experiments show that endogenous 5-HT is a powerful modulator of physiological IHMN activity. This effect appears to be mediated primarily by postsynaptic 5-HT_{2A} receptors and consists of gain modulation of the neuronal discharge pattern via an increase in membrane resistance together with a relative depolarization. An increase in

membrane resistance increases the excitability of the neuron to synaptic inputs, while a relative depolarization moves the membrane potential closer to the firing threshold and thus increases excitation of the neuron.

Acknowledgements

The authors are indebted to Jack Tomlinson (Biology Laboratory Technician, Clement J. Zablocki VA Medical Center, Milwaukee, WI) for outstanding surgical and technical assistance. This work was supported by a National Institute of General Medical Sciences Grant (3 R01 GM059234-05S1) (E.A.E.S.), by the Department of Veterans Affairs Medical Research Funds (E.J.Z.), and by the Department of Anesthesiology of The Medical College of Wisconsin, Milwaukee, WI.

References

Aldes LD, Chapman ME, Chronister RB, Haycock JW. Sources of noradrenergic afferents to the hypoglossal nucleus in the rat. Brain Res Bull 1992;29:931–942. [PubMed: 1282080]

Anderson JW, Sant'Ambrogio FB, Orani GP, Sant'Ambrogio G, Mathew OP. Carbon dioxide-responsive laryngeal receptors in the dog. Respir Physiol 1990;82:217–226. [PubMed: 2127467]

Bayliss DA, Viana F, Talley EM, Berger AJ. Neuromodulation of hypoglossal motoneurons: cellular and developmental mechanisms. Respir Physiol 1997;110:139–150. [PubMed: 9407607]

Berger AJ, Bayliss DA, Viana F. Modulation of neonatal rat hypoglossal motoneuron excitability by serotonin. Neurosci Lett 1992;143:164–168. [PubMed: 1436663]

Brandes IF, Dean C, Jakovcevic D, Stucke AG, Hopp FA, Zuperku EJ, Stuth EA. Anatomical location of genioglossus motoneurons within the adult canine hypoglossal motor nucleus. FASEB J 2004a;D 561:468.7.

Brandes IF, Stuth EAE, Javcovcevic D, Kampine JP, and Zuperku EJ Subanesthetic Concentrations of Isoflurane (ISO) Depress Inspiratory Hypoglossal Motoneurons (HMNs) and their Response to Serotonin. *Anesthesiology* Accepted Abstracts 2004 Annual Meeting, 2004b.

Dhonneur G, Combes X, Leroux B, Duvaldestin P. Postoperative obstructive apnea. Anesth Analg 1999;89:762–767. [PubMed: 10475322]

Dogas Z, Krolo M, Stuth EA, Tonkovic-Capin M, Hopp FA, McCrimmon DR, Zuperku EJ. Differential effects of $GABA_A$ receptor antagonists in the control of respiratory neuronal discharge patterns. J Neurophysiol 1998;80:2368–2377. [PubMed: 9819249]

Dreshaj IA, Haxhiu MA, Martin RJ. Role of the medullary raphe nuclei in the respiratory response to CO2. Respir Physiol 1998;111:15–23. [PubMed: 9496468]

Eastwood PR, Szollosi I, Platt PR, Hillman DR. Collapsibility of the upper airway during anesthesia with isoflurane. Anesthesiology 2002;97:786–793. [PubMed: 12357141]

Fenik P, Veasey SC. Pharmacological characterization of serotonergic receptor activity in the hypoglossal nucleus. Am J Respir Crit Care Med 2003;167:563–569. [PubMed: 12406845]

Fenik V, Kubin L, Okabe S, Pack AI, Davies RO. Differential sensitivity of laryngeal and pharyngeal motoneurons to iontophoretic application of serotonin. Neuroscience 1997;81:873–885. [PubMed: 9316035]

Hara K, Harris RA. The anesthetic mechanism of urethane: the effects on neurotransmitter-gated ion channels. Anesth Analg 2002;94:313–318. [PubMed: 11812690]

Horner RL. The neuropharmacology of upper airway motor control in the awake and asleep states: implications for obstructive sleep apnoea. Respir Res 2001;2:286–294. [PubMed: 11686898]

Iscoe S, Beaton M, Duffin J. Chemoreflex thresholds to CO2 in decerebrate cats. Respir Physiol 1998;113:1–10. [PubMed: 9776545]

Jacobs BL, Azmitia EC. Structure and function of the brain serotonin system. Physiol Rev 1992;75:165–229. [PubMed: 1731370]

Jelev A, Sood S, Liu H, Nolan P, Horner RL. Microdialysis perfusion of 5-HT into hypoglossal motor nucleus differentially modulates genioglossus activity across natural sleep-wake states in rats. J Physiol 2001;532:467–481. [PubMed: 11306665]

Joseph V, Dalmaz Y, Cottet-Emard JM, Pequignot JM. Dexamethasone's influence on tyrosine hydroxylase activity in the chemoreflex pathway and on the hypoxic ventilatory response. Pflugers Arch 1998;435:834–839. [PubMed: 9518513]

Kazama T, Ikeda K. Comparison of MAC and the rate of rise of alveolar concentration of sevoflurane with halothane and isoflurane in the dog. Anesthesiology 1988;68:435–437. [PubMed: 3345000]

Krolo M, Stuth EA, Tonkovic-Capin M, Dogas Z, Hopp FA, McCrimmon DR, Zuperku EJ. Differential roles of ionotropic glutamate receptors in canine medullary inspiratory neurons of the ventral respiratory group. J Neurophysiol 1999;82:60–68. [PubMed: 10400935]

Krolo M, Stuth EA, Tonkovic-Capin M, Hopp FA, McCrimmon DR, Zuperku EJ. Relative magnitude of tonic and phasic synaptic excitation of medullary inspiratory neurons in dogs. Am J Physiol Regul Integr Comp Physiol 2000;279:R639–R649. [PubMed: 10938255]

Kubin L, Davies RO, Pack AI. Control of upper airway motoneurons during REM sleep. News Physiol Sci 1998;13:91–97. [PubMed: 11390769]

Kubin L, Reignier C, Tojima H, Taguchi O, Pack AI, Davies RO. Changes in serotonin level in the hypoglossal nucleus region during carbachol-induced atonia. Brain Res 1994;645:291–302. [PubMed: 7520343]

Kubin L, Tojima H, Davies RO, Pack AI. Serotonergic excitatory drive to hypoglossal motoneurons in the decerebrate cat. Neurosci Lett 1992;139:243–248. [PubMed: 1608554]

Manaker S, Tischler LJ. Origin of serotoninergic afferents to the hypoglossal nucleus in the rat. J Comp Neurol 1993;334:466–476. [PubMed: 8376628]

Marwood JF. Influence of alpha 1-adrenoceptor antagonism of ketanserin on the nature of its 5-HT2 receptor antagonism. Clin Exp Pharmacol Physiol 1994;21:955–961. [PubMed: 7736654]

Miki H, Hida W, Shindoh C, Kikuchi Y, Chonan T, Taguchi O, Inoue H, Takishima T. Effects of electrical stimulation of the genioglossus on upper airway resistance in anesthetized dogs. Am Rev Respir Dis 1989;140:1279–1284. [PubMed: 2817589]

Nakayama H, Smith CA, Rodman JR, Skatrud JB, Dempsey JA. Effect of ventilatory drive on carbon dioxide sensitivity below eupnea during sleep. Am J Respir Crit Care Med 2002;165:1251–1260. [PubMed: 11991874]

Nattie EE, Li A, Richerson G, Lappi DA. Medullary serotonergic neurones and adjacent neurones that express neurokinin-1 receptors are both involved in chemoreception in vivo. J Physiol 2004;556:235–253. [PubMed: 14724193]

Nielsen AM, Bisgard GE, Mitchell GS. Phrenic nerve responses to hypoxia and CO_2 in decerebrate dogs. Respir Physiol 1986;65:267–283. [PubMed: 3097770]

Nilsson IM, Sjoerdsma A, Waldenstrom J. Antifibrinolytic activity and metabolism of 6-aminocaproic acid in man. Lancet 1960;1:1322–1326. [PubMed: 14427269]

Parkis MA, Bayliss DA, Berger AJ. Actions of norepinephrine on rat hypoglossal motoneurons. J Neurophysiol 1995;74:1911–1919. [PubMed: 8592184]

Parkis MA, Feldman JL, Robinson DM, Funk GD. Oscillations in endogenous inputs to neurons affect excitability and signal processing. J Neurosci 2003;23:8152–8158. [PubMed: 12954878]

Remmers JE, deGroot WJ, Sauerland EK, Anch AM. Pathogenesis of upper airway occlusion during sleep. J Appl Physiol 1978;44:931–938. [PubMed: 670014]

Richerson GB. Serotonergic neurons as carbon dioxide sensors that maintain pH homeostasis. Nat Rev Neurosci 2004;5:449–461. [PubMed: 15152195]

Risberg B. Fibrinolysis and trauma. Eur Surg Res 1978;10:373–381. [PubMed: 367786]

Sakai M, Matsunaga M, Kubota A, Yamanishi Y, Nishizawa Y. Reduction in excessive muscle tone by selective depletion of serotonin in intercollicularly decerebrated rats. Brain Res 2000;860:104–111. [PubMed: 10727628]

Schwarzacher SW, Pestean A, Gunther S, Ballanyi K. Serotonergic modulation of respiratory motoneurons and interneurons in brainstem slices of perinatal rats. Neuroscience 2002;115:1247–1259. [PubMed: 12453495]

Severson CA, Wang W, Pieribone VA, Dohle CI, Richerson GB. Midbrain serotonergic neurons are central pH chemoreceptors. Nat Neurosci 2003;6:1139–1140. [PubMed: 14517544]

Singer JH, Bellingham MC, Berger AJ. Presynaptic inhibition of glutamatergic synaptic transmission to rat motoneurons by serotonin. J Neurophysiol 1996;76:799–807. [PubMed: 8871200]

Sirois JE, Lie Q, Talley EM, Lynch IIIC, Bayliss DA. The TASK-1 two-pore domain K^+ channel is a molecular substrate for neuronal effects of inhalation anesthetics. J Neurosci 2000;201:6347–6354. [PubMed: 10964940]

Sirois JE, Lynch IIIC, Bayliss DA. Convergent and reciprocal modulation of a leak K+ current and Ih by an inhalational anaesthetic and neurotransmitters in rat brainstem motoneurones. J Physiol 2002;541:717–729. [PubMed: 12068035]

Sood S, Liu X, Liu H, Nolan P, Horner RL. 5-HT at hypoglossal motor nucleus and respiratory control of genioglossus muscle in anesthetized rats. Respir Physiol Neurobiol 2003;138:205–221. [PubMed: 14609511]

Sood S, Morrison JL, Liu H, Horner RL. Role of endogenous serotonin in modulating genioglossus muscle activity in awake and sleeping rats. Am J Respir Crit Care Med 2005;172:1338–1347. [PubMed: 16020803]

Stucke AG, Stuth EAE, Tonkovic-Capin V, Tonkovic-Capin M, Hopp FA, Kampine JP, Zuperku EJ. Effects of halothane and sevoflurane on inhibitory neurotransmission to medullary expiratory neurons in a decerebrate dog model. Anesthesiology 2002;96:955–962. [PubMed: 11964605]

Stuth EAE, Krolo M, Stucke AG, Tonkovic-Capin M, Tonkovic-Capin V, Hopp FA, Kampine JP, Zuperku EJ. Effects of halothane on excitatory neurotransmission to medullary expiratory neurons in a decerebrate dog model. Anesthesiology 2000;93:1474–1481. [PubMed: 11149443]

Takeuchi Y, Kojima M, Matsuura T, Sano Y. Serotonergic innervation on the motoneurons in the mammalian brainstem. Light and electron microscopic immunohistochemistry. Anat Embryol (Berl) 1983;167:321–333. [PubMed: 6625189]

Tonkovic-Capin M, Krolo M, Stuth EAE, Hopp FA, Zuperku EJ. Improved method of canine decerebration. J Appl Physiol 1998;85:747–750. [PubMed: 9688755]

Veasey SC, Fornal CA, Metzler CW, Jacobs BL. Response of serotonergic caudal raphe neurons in relation to specific motor activities in freely moving cats. J Neurosci 1995;15:5346–5359. [PubMed: 7623157]

Wang W, Tiwari JK, Bradley SR, Zaykin RV, Richerson GB. Acidosis-stimulated neurons of the medullary raphe are serotonergic. J Neurophysiol 2001;85:2224–2235. [PubMed: 11353037]

Zuperku EJ, McCrimmon DR. Gain modulation of respiratory neurons. Respir Physiol Neurobiol 2002;131:121–133. [PubMed: 12107000]

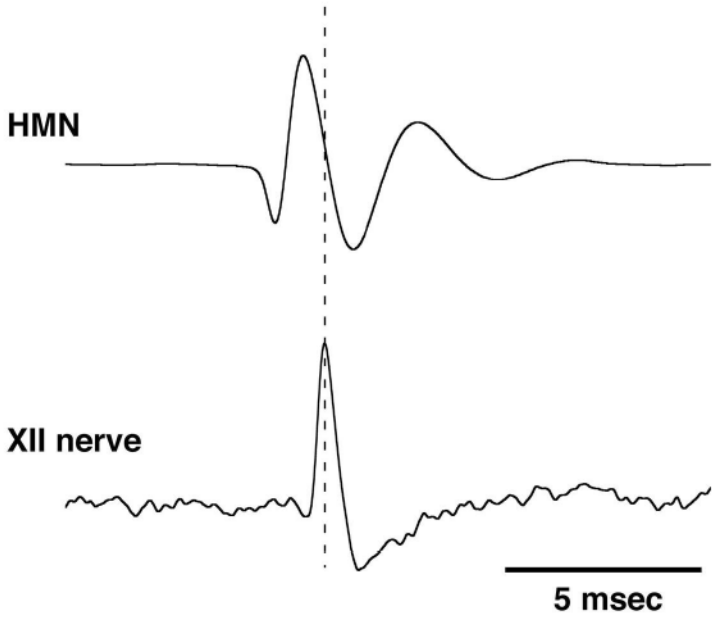

Figure 1.
The presence of an axon spike potential in the spike-triggered average of hypoglossal (XII) nerve activity, delayed relative to a hypoglossal motoneuron (HMN) action potential confirmed that the recorded brainstem neuron was a HMN (500 sweeps/average).

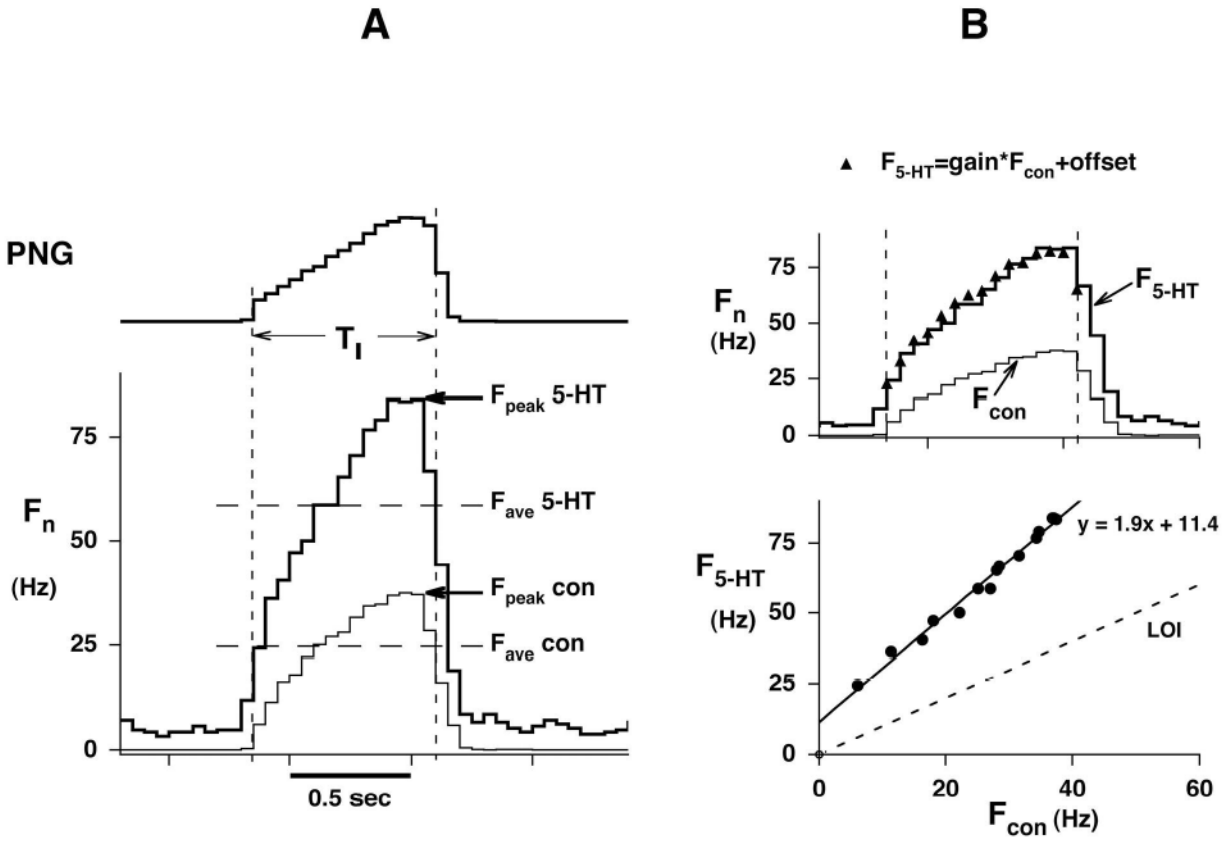

Figure 2.

Analysis of neuronal data using Cycle-Triggered Histograms (CTHs) A: Peak (F_{peak}) and time-averaged (F_{ave}) neuronal discharge frequency before (F_{con}) or during 5-HT ejection ($F_{5\text{-}HT}$). Each graph represents the averaged values of 10–15 respiratory cycles (50 msec bins). PNG: Phrenic neurogram, T_I: inspiratory duration (vertical dashed lines), F_n:neuronal discharge frequency. B, Upper: Analysis period (vertical dotted lines) of the cycle-triggered histograms. B, Lower: Plot of $F_{5\text{-}HT}$ vs. F_{con} shows that the two discharge patterns are linearly related. $F_{5\text{-}HT}$ = slope * F_{con} + y-intercept where the slope (1.90) is the gain and the y-intercept (11.4 Hz) is the offset of the pattern. LOI: Line of identity. Recalculating $F_{5\text{-}HT}$ values from F_{con} with help of the linear regression parameters yields values that closely match the original CTH (superimposed triangles in B, upper).

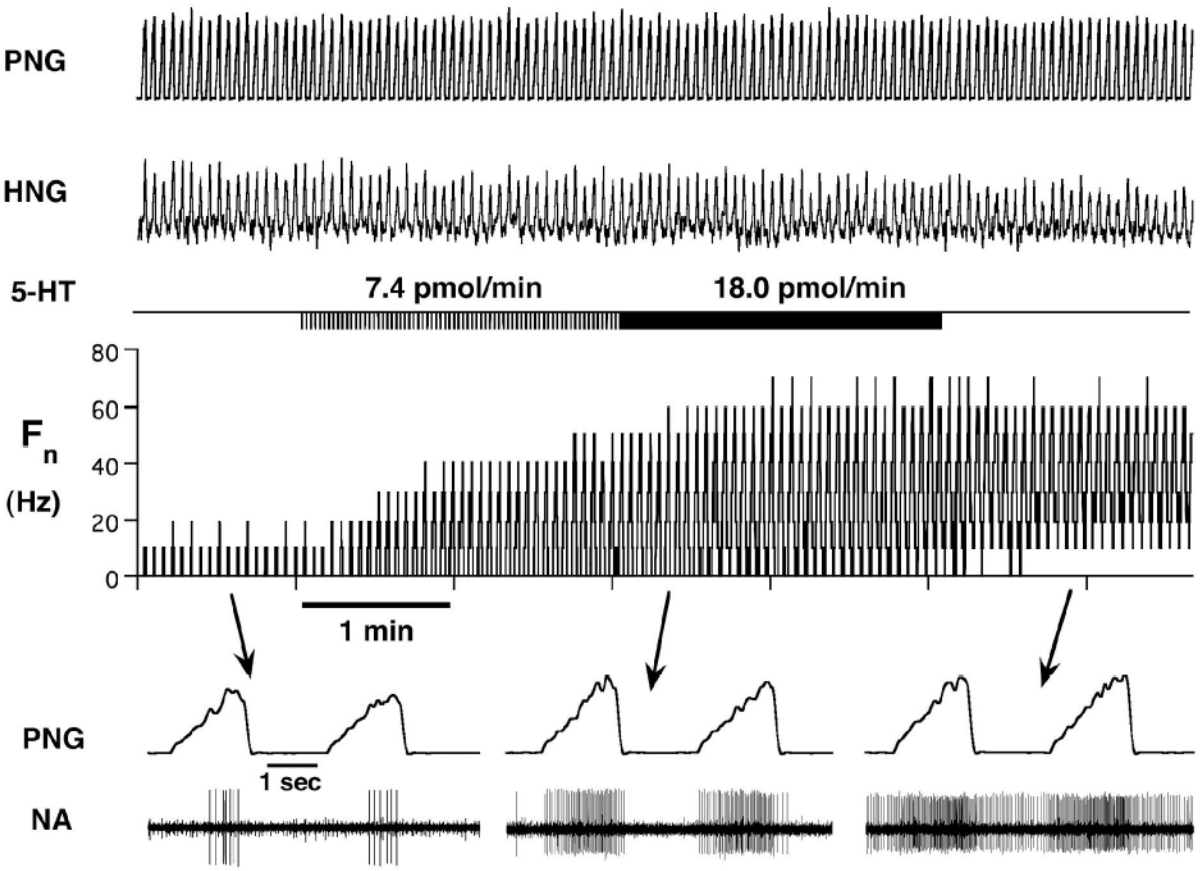

Figure 3.

Response of an inspiratory hypoglossal motoneuron to increasing dose rates of 5-HT. The duration of picoejection is shown (5-HT) and the dose rates are given. The bottom traces show time-expanded views during control conditions and at different 5-HT dose rates. The simultaneously recorded phrenic neurogram identifies this neuron as inspiratory and the positive spike-triggered average (not shown) verifies that this is a HMN. At the intermediate dose rate, the neuron fires throughout the whole inspiratory phase, while at the maximal effective dose rate the neuron also shows activity during the previously silent expiratory phase. PNG: phrenic neurogram, HNG: hypoglossal neurogram, F_n: rate meter of neuronal discharge frequency in Hz, NA: neuronal activity.

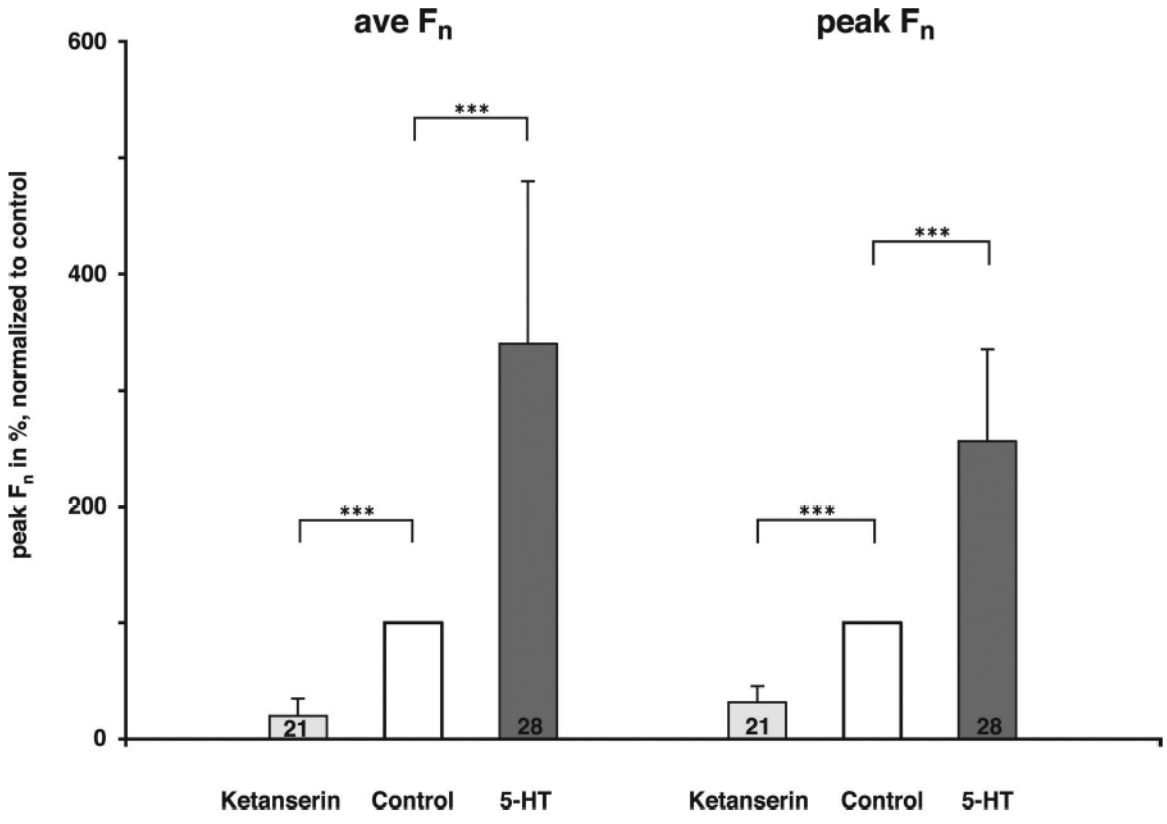

Figure 4.

Comparison of the effect of 5-HT and ketanserin on time-averaged F_n and peak F_n; values are given as mean and SD. The numbers in the bars indicate the number of protocols in each group. At maximally effective dose rates 5-HT increased the time-averaged F_n to 340 % (SD 140) and the peak F_n to 256 % (SD 79); whereas, ketanserin decreased the time-averaged F_n by 80 % (SD 15) and the peak F_n by 68 % (SD 15). ***: $p < 0.001$.

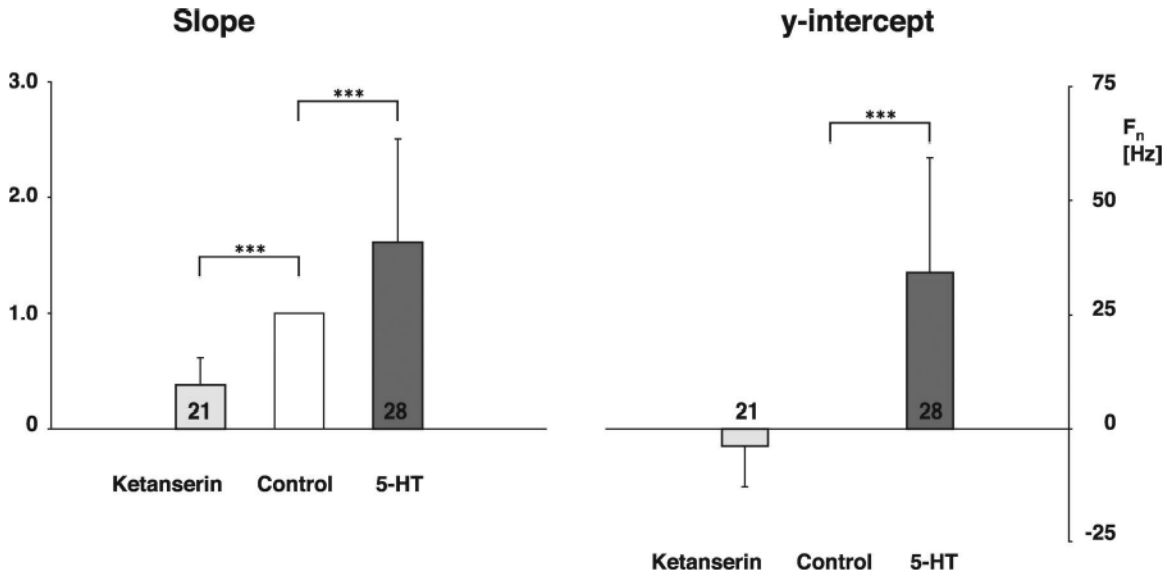

Figure 5.

Effect of 5-HT and ketanserin on the slope and the y-intercept of the relationship between the neuronal discharge patterns for the control and maximal effective drug dose rates. 5-HT increased the slope of the neuronal discharge pattern by 61 % (SD 89); whereas, ketanserin caused a decrease of 63 % (SD 24). 5-HT shifted the y-intercept by 34 Hz (SD 26) and ketanserin reduced the y-intercept by 4 Hz (SD 9). Values are given as mean and SD. Numbers in the bars indicate the number of protocols per group. ***: $p < 0.001$.

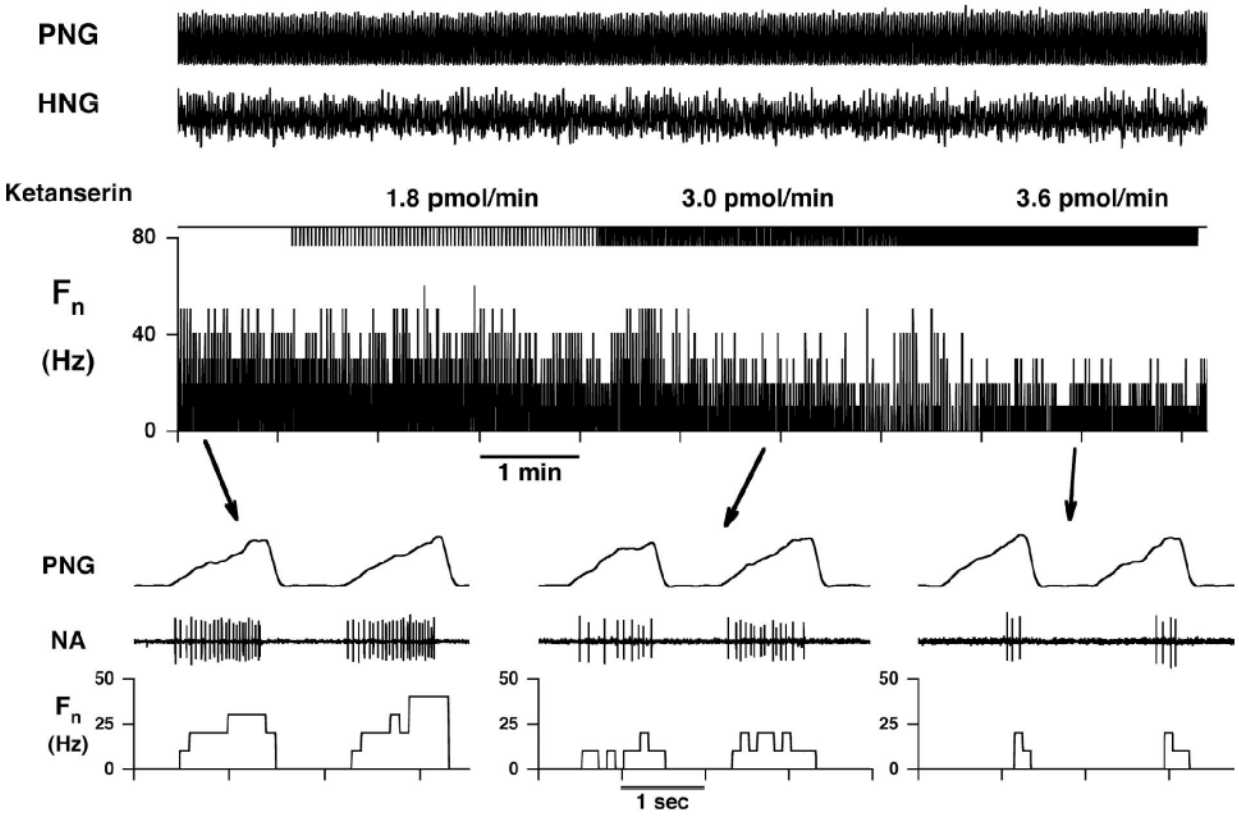

Figure 6.

Response of an inspiratory hypoglossal motoneuron to increasing dose rates of ketanserin. The duration of picoejection is marked (ketanserin) and the dose rates are given. The bottom traces show time-expanded views. The simultaneously recorded phrenic neurogram identifies this neuron as inspiratory. PNG: phrenic neurogram, HNG: hypoglossal neurogram, F_n: rate meter of neuronal discharge frequency in Hz, NA: neuronal activity.

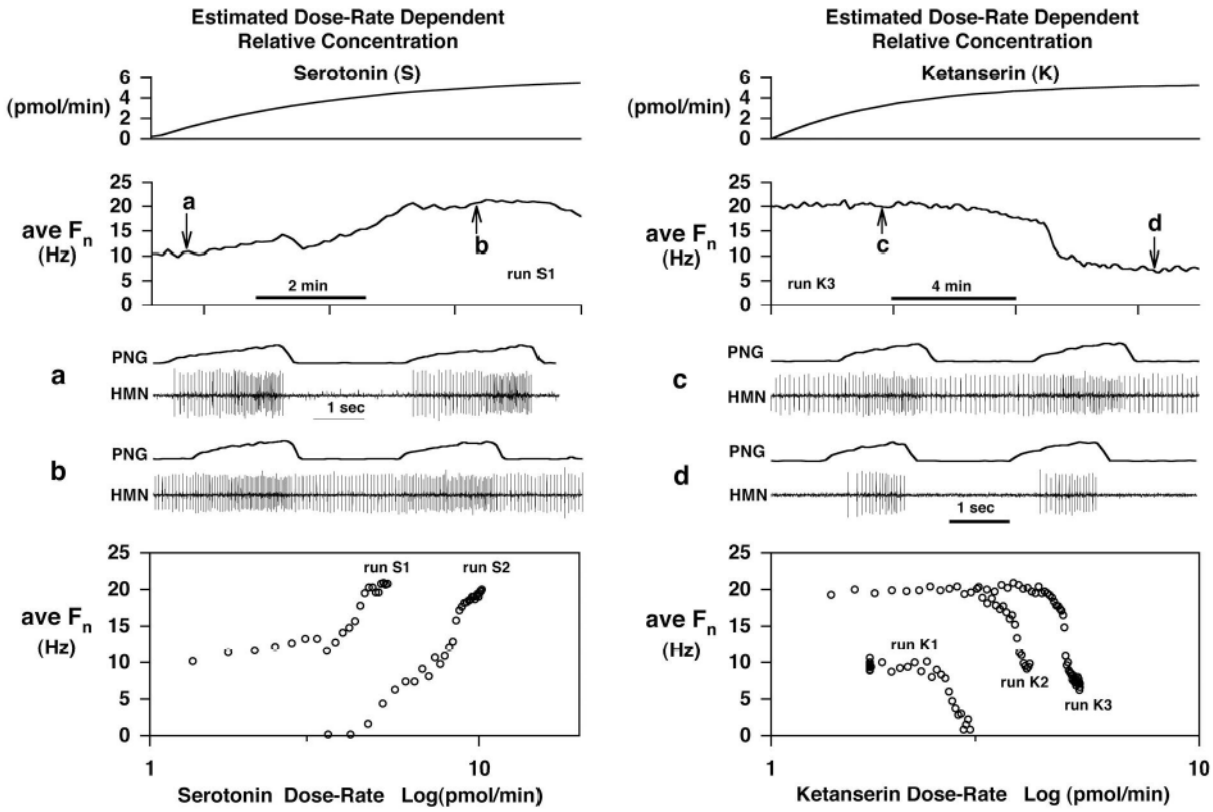

Figure 7.

Competitive antagonism between serotonin (S) and the serotonin antagonist ketanserin (K). An inspiratory hypoglossal motoneuron was sequentially exposed to S and K to show that K competitively blocks serotonergic activation of the neuron. The left and right panels show agonist and antagonist data, respectively. From top to bottom the estimated relative drug concentration, the average F_n /respiratory-cycle duration, two time-expanded views of the neuron activity, and finally plots of average F_n vs. log of the relative concentration are shown. The estimated relative concentrations are related to the dose rate, where continuous picoejection at a constant rate is initiated at time zero. Due to diffusion properties, the relative concentration (C_R) increases asymptotically, i.e., C_R = dose rate *[1-exp(-t/180 sec)], to a level that is proportional to the picoejection dose rate. The agonist and antagonist were applied in the following sequence S1→K1→S2→S2&K2→S2&K3. Numbers indicate run number. The bottom graphs demonstrate competitive antagonism between S and K. Picoejection of S increased ave F_n (S1; 6.1 pmol/min). After recovery from S, K antagonism resulted in silencing of the neuronal activity (K1; 3.4 pmol/min)). During the K block, significantly higher S rates (10.8 pmol/min) were required to overcome the competitive K antagonism as demonstrated by the right shift of the S2 curve. Once S reversed the K block, the peak S dose rate was maintained and an increased K rate (4.5 pmol/min) resulted in competitive antagonism (K2), which was overcome by an increase in the ongoing S rate (15.3 pmol/min) once the K2 run was terminated. A further parallel shift in antagonist dose rate (K3; 5.4 pmol/min) occurred during the ongoing S2 dose rate (15.3 pmol/min).

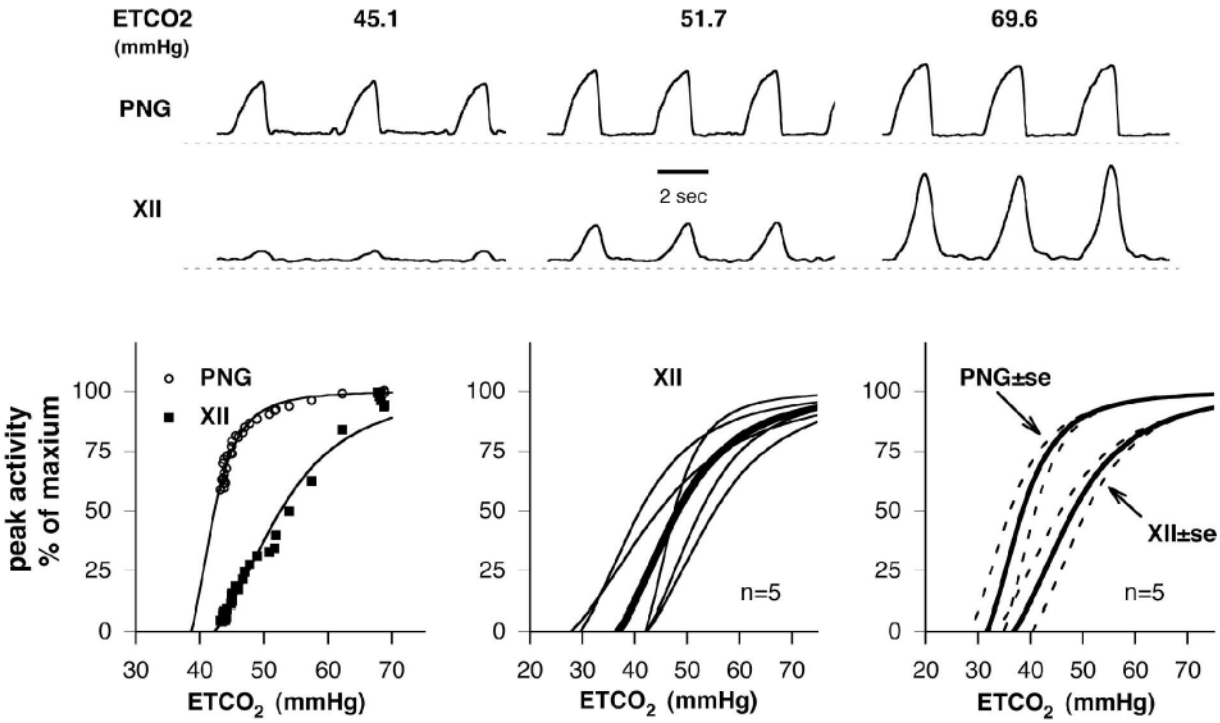

Figure 8.

CO_2 responses of phrenic nerve and XII nerve activities in hyperoxic decerebrate dogs. Upper: Example of the effects of CO_2, measured as end-tidal $ETCO_2$ (mmHg), on the moving-time averages of phrenic nerve activity (PNG, top trace) and XII nerve activity (XII, 2nd trace). Lower Left: plot of normalized peak activity vs. $ETCO_2$ associated with the example from the upper traces. Nonlinear regression was used to fit both nerve activity plots and to aid in extrapolating the apneic thresholds. A hyperbolic function of the form: $Y=(X-\varphi)^3/[(X-\varphi)^3+(X_o-\varphi)^3)]$ was used, where Y is peak activity, X is $ETCO_2$, φ is $ETCO_2$-axis intercept and X_o is the $ETCO_2$ level for 50% of maximum peak activity. The response curve for XII activity is shifted to the right and shallower with a greater linear range compared to the phrenic activity. The apneic thresholds are ~38 and ~42 mmHg for the phrenic and XII activities, respectively. An $ETCO_2$ of ~52 mmHg produced a peak XII activity of 50% of maximum. Lower center: XII nerve activity vs. $ETCO_2$ plots for five dogs (thin lines) and group mean curve (thick line). In three of five animals there was no XII activity below an $ETCO_2$ of 42 mmHg. Lower right: mean curves ± 1 SE bands of both activities. The XII nerve activity curve was consistently right shifted and shallower than the phrenic response curve. $ETCO_2$ levels of 65–70 mmHg were required to produce maximal XII activity. $ETCO_2$ levels required for 50% of maximum ranged from 41–55 mmHg (center plots).